# Variable Activation Energy to Model Oil Shale Pyrolysis Kinetics

*Omar S. Al-Ayed*[†] *and Sulieman Q. Abu Ein*
Faculty of Engineering Technology, Al-Balqa Applied University, Marka, Jordan
[†]e-mail: osalayed@fet.edu.jo

## *Abstract*

Fixed bed experimental runs are used to model the kinetics of total weight loss of Ellajjun oil shale. Samples of 400g are used in the study at 350 – 550 $^{o}$C temperatures and heating rate $h$ in the range of 2.6 to 11 $^{o}$Cmin$^{-1}$. The total weight loss of the oil shale is fitted to standard first order kinetic model encompasses heating rate and variable activation energy as function of conversion.

$$\ln\left[-\ln(1-x)\right] = \ln\left\{\left(\frac{k_o RT}{hE(x)}\right)\left(1-\frac{2RT}{E(x)}\right)\right\} - \frac{E(x)}{RT}$$

Where, $x$ is defined as difference in weights of fresh charged sample and spent shale at the end of run divided by fresh sample weight. This result is in agreement with other researchers who modeled the TGA and DGA kinetic data with variable activation energies depending upon number of reactions involved.

Rate of liquid accumulation from fixed bed retort also has been modeled using a second order kinetics in which activation energy is taken constant:

$$\frac{dw_l}{dt} = k_{ol}\exp\left(-\frac{E_l}{RT}\right)(1-w_l)^2$$

where $w_l$ is defined as total accumulated weight of liquid at any time divided by total liquid collected at the end of run.

## *Introduction*

Numerous researchers (Charlesworth, 1985; Braun and Rothman, 1975; Skala,et al., 1987, 1990; Johannes, et al., 2006, 2007; Campbell et al., 1980b; Torrente and Galan, 2001) have investigated the decomposition kinetics of oil shale. Most of the reported modeling studies are based on TGA, DGA, DSC and Rock-Eval Analyzer results. The obtained data combined with different mathematical procedures for determining kinetic parameters. Integral and differential methods, the method of maximum rate have been used. Varieties of kinetic models have been employed to fit experimental data to describe the rate of generation of pyrolysis products. These models have been either complex in nature; utilizing intermediates formed from kerogen decomposition and its further transformation into oil and gaseous produce or have assumed a first-order depletion of kerogen. Allred (1966) has reported that the process of oil evolution during oil shale pyrolysis can be regarded as the sum of two separate steps. The first involves degradation and the second is the evaporation of the products, with activation energies of 46 and 39 kJ mol$^{-1}$, respectively. As the temperature increased, this latter process is claimed to be the rate-determining step. Wall et al. (1970) have measured the rates of molecular vaporization of several pure linear alkanes**.** They report that the kinetics is zero order throughout and that the energy of evaporation is proportional to the two-thirds power of the number of carbon atoms. Braun and Rothman (1975) reported 44.6 kJmol$^{-1}$ activation energy below 760K reaction temperature for decomposition of bitumen involves breaking

of relatively weak chemical bonds, while higher activation energy, 177.6 $kJmol^{-1}$ involves breaking of kerogen much stronger chemical bonds.

The weight loss in the low temperature pyrolysis region is attributed to the loss of moisture, interlayer water and the decomposition of mineral nahcolite ($NaHCO_3$) which takes place upto 120 $^oC$ (Qing, et al. 2007). Physical changes, such as softening and molecular rearrangement that associated with the release of gases and structural water also have been reported (Jaber and Probert, 1999) at temperatures lower than 500 $^oC$. The peak occurring early in the vapor is attributed to the rapid evaporation of the organic material not chemically bonded to the kerogen network.

Campbell et al. (1980a) studied the rate of evolution of $CH_4$, $H_2$, CO, $CO_2$, and $C_2$, $C_3$ hydrocarbons during pyrolysis of Colorado Oil Shale at linear heating rates varying from 0.5 to 4.0$^oCmin^{-1}$. These workers reported 11 $cm^3g^{-1}$ of hydrogen gas with a corresponding hydrogen peak at 455 $^oC$. More of hydrogen release was reported at lower heating rates. Traces of carbon dioxide and carbon monoxide are detected below 550 $^oC$. Methane formation and evolution initiated at temperature slightly lower than 350 $^oC$ and reaching a maximum value at 445 $^oC$. The production of $CH_4$ continues to about 750 $^oC$ and the estimated amount produced was 3.5 $cm^3g^{-1}$ .Rate of methane release increased with decreasing heating rate. Ethane and ethene ($C_2$) production increased to a maximum value at 450 $^oC$ and stopped at slightly higher than 550 $^oC$. $C_3$ (propane and propene) 0.53 $cm^3g^{-1}$ are produced. The maximum value of production is found to occur at 450 $^oC$ and the formation of $C_3$ is stopped at 525 $^oC$. Oil release profile is corresponding closely to that observed for $C_1$ and $C_2$ profiles. In addition, Dawsonite, $NaAl(OH)_2CO_3$ decomposes to $Na_2CO_3$ , $Al_2O_3$ , $H_2O$ , $CO_2$ between 350- 400 $^oC$

The decomposition of the oil shale involves a large number of reactions in parallel and in series, whilst TGA measures the overall weight loss due to these reactions. A combined study (Bhargava, et al., 2005) using TGA, DRIFTS, and XRD resulted in a better insight to oil shale reactions. TGA provides general information on the overall reaction kinetics rather the individual reactions. Therefore activation energies derived from TGA data are apparent activation energies.

Li and Yue (2003) studied the pyrolysis kinetics of different Chinese oil shale samples at a constant heating rate of 5$^oCmin^{-1}$. The TGA data obtained used to develop a kinetic model which assumes 11 first order parallel reactions with changed activation energies and frequency factors. These workers have reported apparent activation energies in 80 -280 $kJmol^{-1}$ range and apparent frequency factor in the range $1.3*10^4$ to $1.4*10^{19}$ . The calculated fractional conversion of each reaction is a complex function of activation energy. Pyrolysis reactions with low activation energies, the pyrolysates of oil shale result mainly form the rupture of weak chemical bond, probably the rupture of weak cross linked bonds, such as, C-O bond, C-S bond, (Djurcic, et al., 1971; Young and Ken, 1971). Also, rupture of branched functional groups in kerogen long molecular structure. These weak bonds have low rupture energy which commensurate with pyrolysis gaseous products such as $H_2O$, $CO_2$, $H_2S$, $H_2$ and light hydrocarbons. The medium activation energy values are associated with break up of the side chains in β-site of aromatics, decomposition of normal alkane with large molecular weight, Diels-Alder cyclation reaction and the rupture of alicyclic hydrocarbon. This corresponds to pyrolysis temperature between 420 – 480 $^oC$. On the other hand, pyrolysis reactions with the high apparent activation energies are mainly the aromatization of alicyclic compounds, dehydrogenation and combination of aromatic rings, rupture of heterocyclic compounds. As it has been discussed above that kerogen decomposition to produced oil shale and gases is a continuous process composes of several parallel, series, simultaneous and complex reactions nature.

*Experimental Setup*

Oil shale samples from Ellajjun area located in the southern region of Jordan were studied and investigated in this work.

The original oil shale samples, were ground in a ball mill, and sieved to particles size 0.9 - 2.8 mm. The size selection based on diffusional influences and mass transfer studies. All samples washed with water and dried to reduce dust and fine particles.

All experiments were conducted in a stainless steel fixed bed retort. Four hundred gram of oil shale sample was electrically heated in a 70 mm diameter and 300 mm length cylindrical retort. Reactor and furnace temperatures were controlled to obtain the desired retorting temperature. The type K thermocouple inserted from the top of retort to the middle point of oil shale sample for monitoring reaction temperature, while the other thermocouple was fixed between the external body of the retort and the inner side of the heater wrapped ceramic cylinder for controlling the heat input and subsequent the retort temperature. The surrounding temperature of the retort was kept higher than the retort desired temperature to avoid time lag. Nitrogen sweep gas introduced from the top side of the retort for preheating while passing downward to the bottom of the retort, and then allowed to disperse to sweep the generated products upward to upper outlet. Oven temperature controlled and monitored by digital temperature controller indicated as Oven temperature controller T.C. in figure 1.

The generated hydrocarbon is driven out by virtue of $N_2$ sweep gas to pass through a glass condenser. The circulating coolant is maintained at 2 $^oC$ ± 2 to condense the liquid hydrocarbons that are condensable while the light organic and non-organic gases were vented. The experimental work has been conducted in two sections:

1- *Total Weight Loss Measurement.*

In order to measure the total weight loss of sample as function of reaction temperature, several runs were conducted at 350, 370, 390, 410, 430, 450, 470, 490, 510, 530, and 550 $^oC$ temperatures. The difference in sample weights before and after pyrolyzing at the desired temperature was taken as total weight loss and used for kinetics modeling. After retort heater switched off, retort was subjected to fast external cooling with help of two air compressors to stop further increase in retort temperature and prevent reaction of kerogen.

2- *Heating Rate Measurement.*

Weight of condensed liquids of oil shale and water recorded as function of time and heating rate for rate of liquid accumulation modeling. Rate of liquid oil accumulation and water and heating rate were recorded as function of time using a digital balance with 0.01 g least reading accuracy. Heating rate was obtained and controlled to the desired level with help of variable heat input instrument.

Fischer Assay analysis was conducted in

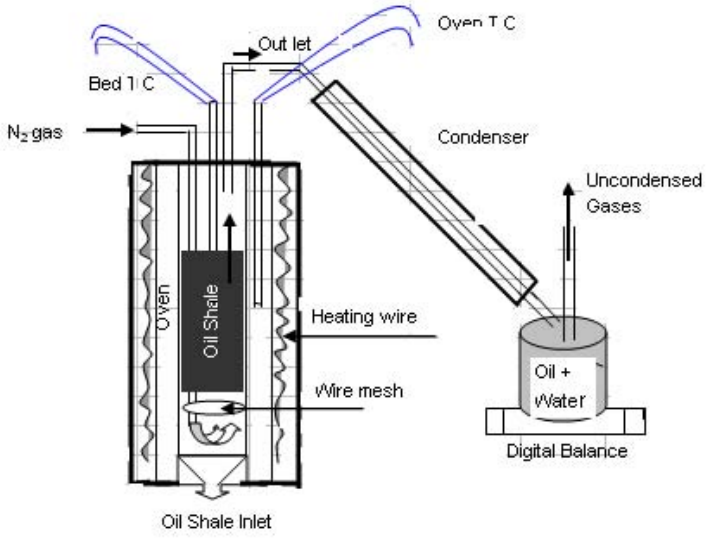


Figure 1: Experimental Setup Diagram

the laboratories of Natural Resources Authority, Jordan. The results indicated that 12.2% weight of the tested sample is shale oil.

Oil shale total weight loss and liquids of shale oil produced investigated in 623 - 823 K temperatures range. Heating rates, ($h$), in the range 2.6 – 13.0$^{o}$C$min^{-1}$, were investigated during the entire experimental temperature range.

## *Results and Discussion*

Investigations (Arvo Ots, 2004) have shown that activation energy of oil shale char oxidation depends on the ratio of C/H in char. The value of activation energy, E increased with a decrease in C/H ratio. Chemical composition, phase state, and relative content of the components of volatile matter are determined by the type and location of functional groups of compounds in a molecule of fuel organic matter. During thermal decomposition, hydrocarbons ($CH_4$, $C_2H_2$, $C_2H_6$ and others) form from aliphatic compounds, $CO_2$ is released from the carbonyl group; carbon monoxide arises from ethers, and water from the hydroxyl group. Chemical interactions have been observed to take place between volatile compounds form during thermal decomposition of fuel both within the particle and also in the surrounding medium.

Ellajjun Oil shale showed (Jordan NRA, 2007] marked absorption of heat upto about 400$^{o}$C. This may be related to volatile distillation, for such products appeared at this temperature. From 400 to 460 $^{o}$C the reaction is practically neutral. These neutral reactions zone is followed by sudden exothermic reactions beginning at 460 $^{o}$C and continuing to higher temperatures. In the temperature range 150 – 550 $^{o}$C, release of hydrocarbons by thermal cracking of kerogen which is considered exothermic reactions, in addition to the evolution of hydrocarbon in this temperature range, roasting of pyrites which is completed at 520 $^{o}$C and dehydration of phosphate complex is also taking place in the 480 – 520 $^{o}$C range. In the 150 – 550 $^{o}$C temperature range, parallel and series reaction of hydrocarbons are diagnosed to take place and production of liquid and gas forming components. Release of absorbed water, volatile materials are accompanied production of hydrocarbons in this active region which extend to 550 $^{o}$C. Close to 550 $^{o}$C temperature, reactions favoring hydrocarbons gases formation are augmented as a result of catalytic effect of some components present in the spent ash which adds to the complexity of pyrolysis reactions of oil shale. To account for a collective group of reactions simultaneously, variable activation energy principal is more appropriate to consider and apply rather than apparent activation energy. High apparent activation energies are mainly the aromatization of alicyclic compounds, dehydrogenation and combination of aromatic rings, rupture of heterocyclic compounds coke formation reactions. As it can be seen that variable activation model is more appropriate to model the decomposition reaction kinetics of oil shale. Oil Shale is peculiar in nature and different from all other normal chemical reactions.

## *Kinetic Modeling*

*a) Total Weight Loss:* Ellajjun oil shale kinetics and characteristics has been studied by several researchers (Jaber and Probert, 1999; Nazzal, 2002). In this work, a different approach has been adopted to model the Ellajjun oil shale kinetics. As it can be seen from figure 2 that increasing the pyrolysis temperature increase the total weight percent loss and liquid accumulation while production of gases passes through a maximum. Such results have been observed by other workers (Campbell et al., 1980a). The liquid accumulated composes of both intermolecular and structural waters and hydrocarbons. The amount of bounded water and structural water was determined in a special run and it was estimated to be 1.9% wt. while moisture content was estimated to be 1.2% wt. The maximum total weight loss was 23% recorded at 550 $^{o}$C temperature. On the other hand liquid collected was 50% of estimated Fischer Assay which indicated 12.2% oil. Gaseous amount was

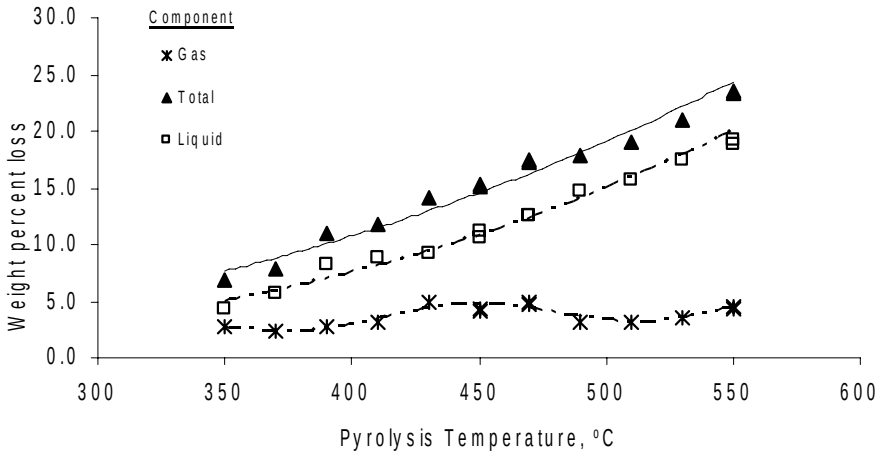


Figure 2 Effect of pyrolysis temperature on weight loss

calculated by difference since nitrogen was flow at less than 50 $cm^3min^{-1}$. The total weight loss data obtained at various pyrolysis temperatures were fitted to a first order rate equation:

$$\frac{dx}{dt} = k(1-x) \qquad \{1\}$$

Where: $x$ is the ratio of weight of sample at the end of run divided by the initial feed in gram fed to reactor. Reaction rate constant $k$ is function of pyrolysis temperature and $dx/dt$ is the rate of weight loss at any time during experimental run. Equation {1} can be re-written after introducing heating rate, $h = dT/dt$, $^oCmin^{-1}$ to give:

$$\frac{dx}{dT} = \frac{k_o}{h}\exp(-E/RT)(1-x) \qquad \{2\}$$

Expanding the exponential function and

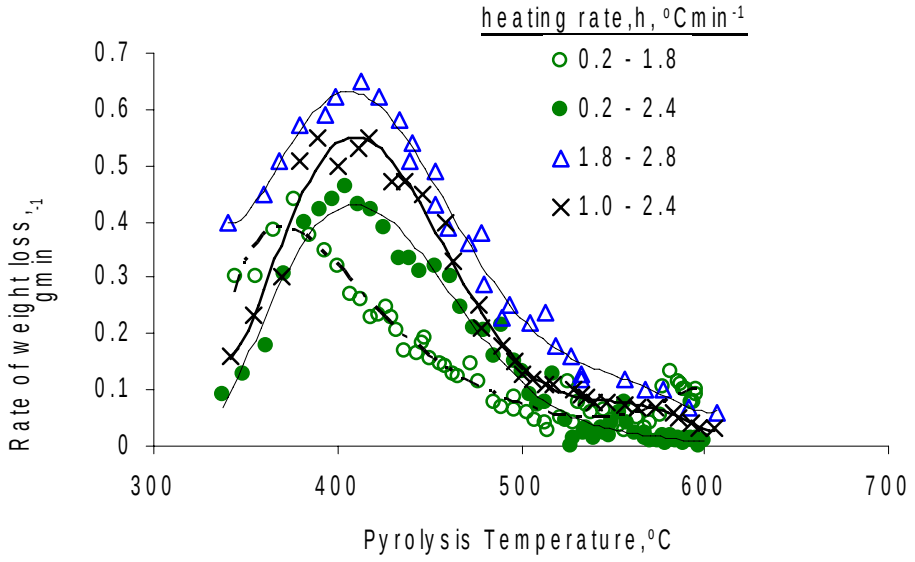


Figure 3: Effect of heating rate on the rate of liquid accumulation as function of temperature

truncation of higher terms, then integrating, equation {2} to obtain:

$$\ln\left[-\ln(1-x)\right] = \ln\left[\frac{k_o RT^2}{hE}\left(1-\frac{2RT}{E}\right)\right] - \frac{E}{RT} \quad \{3\}$$

Equation {3} is used to model the total weight loss data and the results are shown in figure 4. The fit as indicated in the figure is a result of 105 kJmol$^{-1}$ value of activation energy and the corresponding $9.15*10^5$ magnitude of frequency factor. Modifying the activation energy term to be a function of total weight loss percent, $x$, as:

$$E(x) = E_o(1+x) \quad \{4\}$$

Where: $E_o$ = 98kJmol$^{-1}$

This value resulted in a better fit and equation {3} can be written as:

$$\ln\left[-\ln(1-x)\right] = \ln\left[\frac{k_o RT^2}{hE(x)}\left(1-\frac{2RT}{E(x)}\right)\right] - \frac{E(x)}{RT} \quad \{5\}$$

This constant value of activation energy in equation {3} is modified in magnitude to be 98 kJmol$^{-1}$. Since $E(x)$ is function of conversion and will increase with increasing decomposition of kerogen to higher value.

The result of introducing variable activation energy principal as indicated by equation {4} into equation {3} to obtain equation {5} has improved the fit immensely as shown in figure 5. As it can be seen from figure 5, that the predicted values of the function $\ln(-\ln(1-x))$ is excellent when the initial activation energy, $E_o$ value is 98kJmol$^{-1}$ and increased to a final value of $1.2*10^3$ kJmol$^{-1}$ as function of conversion. The constant apparent activation energy value of 105 kJmol$^{-1}$ is average value between the initial and final magnitudes of $E(x)$. The arguments presented in the introduction of this research work attempted to explain the exigency of applying the principal of variable activation energy. Since oil shale characteristics and properties are different from normal chemical reactants, it is imperative to alienate modeling of reaction kinetics away from the normal standard work. The inability of changing reactants concentration during run, and inherent effect of the inorganic portion of the constituents and its influence on reaction kinetics makes oil shale an entity by itself.

*b) Liquid Accumulation:* During runs, the rate of liquid accumulation was measured. The kinetics of liquid accumulation was

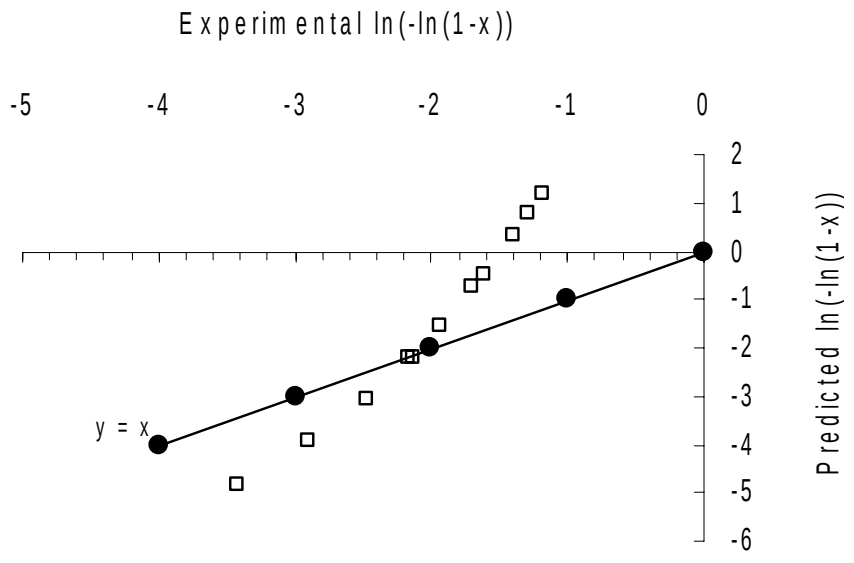


Figure 4: Experimental and theoretical $\ln(-\ln(1-x))$ with constant activation energy.

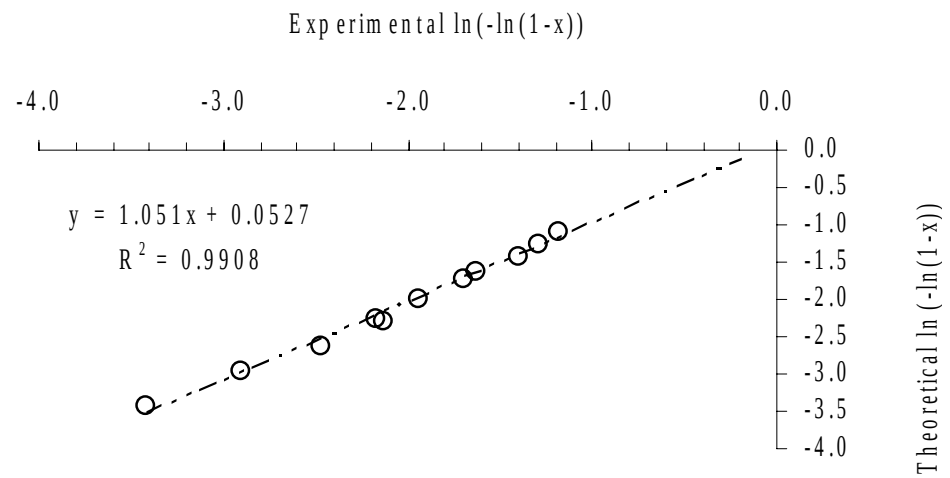


Figure 5: Experimental and theoretical $\ln(-\ln(1-x))$ with variable activation energy.

modeled using a second order equation of the form:

$$\frac{dw_l}{dt} = k_{ol} \exp\left(-\frac{E_l}{RT}\right)(1-w_l)^2 \qquad \{6\}$$

Where $\frac{dw_l}{dt}$ is rate of liquid accumulation during the run in which $w_l$ is defined as $w_t / w_\infty$. The term $w_t$ is the amount of liquid accumulated at any time during run whereas $w_\infty$ is the total liquid accumulated at the end of each run. $k_{ol}$ is the pre-exponential factor for liquid generation rate. Figures 6, 7 and 8 show the comparison of experimental rate of liquid accumulation and the predicted values for different heating rate. As it can be seen from the figures that a good fit is achieved and the error is reduced farther with higher heating rates. A second order equation used to model the rate of liquid accumulation with a constant activation energy equal to 76.5 kJmol$^{-1}$ while the magnitude of the $k_{ol}$ is estimated to be $1.16*10^4$. The reported values of this work are close in range to the lower side of the estimated values by Li and Yue (2003).

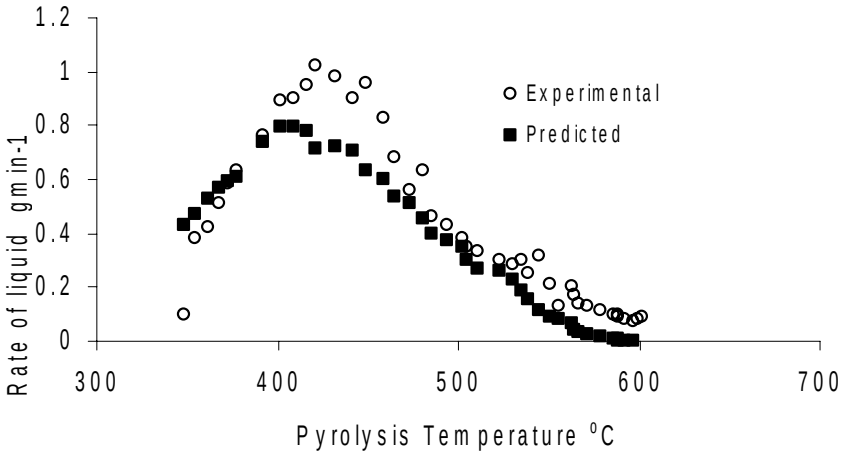


Figure 6: Comparison of predicted and experimental rates at heating rate, 4 $^{o}$Cmin$^{-1}$

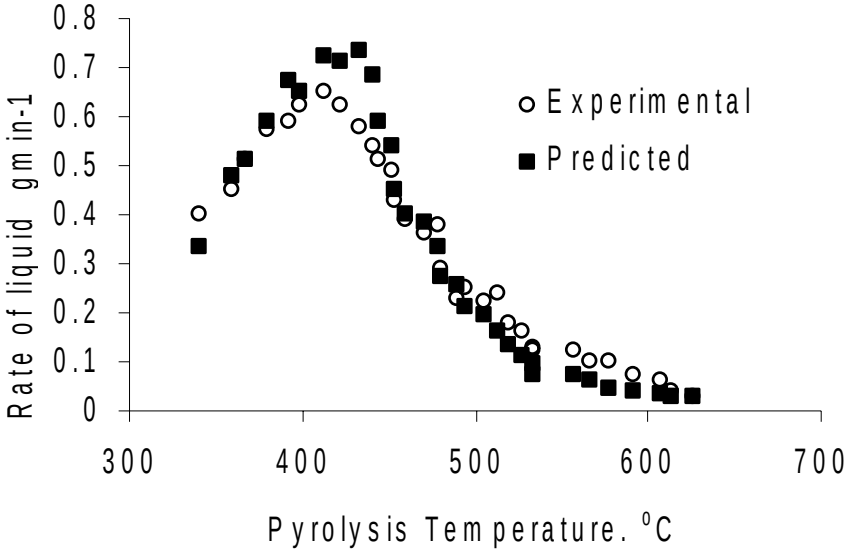


Figure 7: Comparison of predicted and experimental rates at heating rate 2.2 $^{o}Cmin^{-1}$

*Conclusions*

A first order reaction model was developed which assumes variable activation energy and constant frequency factor to describe the oil shale pyrolysis. By using this model, the kinetic parameters were determined based on fixed bed retort. The total weight percent loss data were modeled for Jordanian oil shale from Ellajjun area. The fit of the model to the experimental data is excellent.

Another model of second order kinetics was developed that assumes constant activation energy for predicting the rate of liquid accumulation during the run. The fit of the model to the experimental data is improved with increasing the heating rate.

*References*

Allred, V. D., 1966, Kinetics of oil shale pyrolysis: Chemical Engineering Progress, v. 62, p. 55-60.

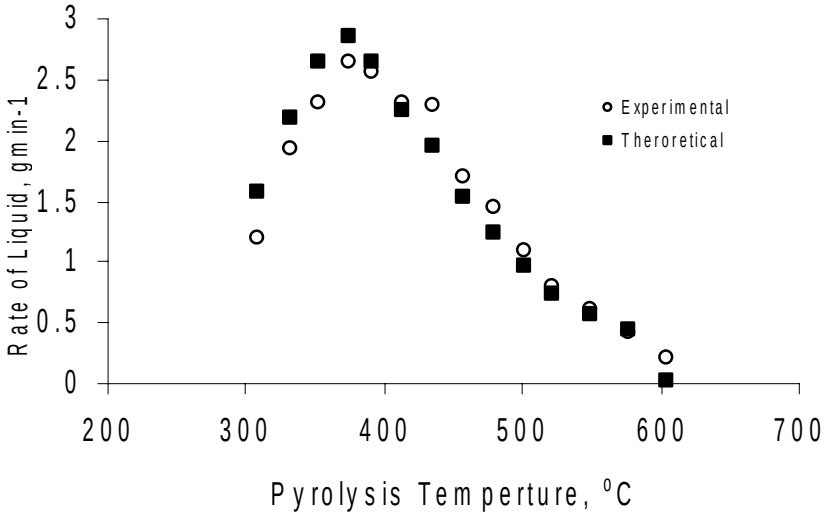


Figure 8: Comparison of predicted and experimental rates at heating rate 11 $^{o}Cmin^{-1}$

Bhargava, S., F. Awaja, and N. D. Subasinghe, 2005, Characterisation of some Australian oil shale using thermal, X-ray and IR techniques: Fuel, v. 84, p. 707-715.

Braun, R. L., and A. J. Rothman, 1975, Oil-Shale pyrolysis: Kinetics and mechanism of oil production: Fuel, v. 54, p. 129-131.

Campbell, J. H., G. Gallegos, and M. Gregg, 1980a, Gas evolution during oil-shale pyrolysis. 2. Kinetic and Stoichiometric analysis: Fuel, v. 59, p. 727-732.

Campbell, J. H., G. J. Koskinas, G. Gallegos, and M. Gregg, 1980b, Gas evolution during oil-shale pyrolysis. 1. Non-isothermal rate measurements: Fuel, v. 59, p. 718-726.

Charlesworth, J. M., 1985, Oil-shale pyrolysis. 2. Kinetics and mechanism of hydrocarbon evolution: Industrial & Engineering Chemistry Process Design and Development, v. 24, p. 1125-1132.

Djuricic, M., R. C. Murphy, D. Vitorovic, and K. Biemann, 1971, Organic acids obtained by alkaline permanganate oxidation of kerogen from the Green River (Colorado) shale: Geochimica et Cosmochimica Acta, v. 35, p. 1201-1207.

Jaber, J. O., and S. D. Probert, 1999, Pyrolysis and gasification kinetics of Jordanian oil-shales: Applied Energy, v. 63, p. 269-286.

Johannes, I., K. Kruusement, and R. Veski, 2007, Evaluation of oil potential and pyrolysis kinetics of renewable fuel and shale samples by Rock-Eval analyzer: Journal of Analytical and Applied Pyrolysis, v. 79, p. 183-190.

Johannes, I., K. Kruusement, R. Veski, and J. A. Bojesen-Koefoed, 2006, Characterisation of pyrolysis kinetics by Rock-Eval basic data: Oil Shale, v. 23, p. 249-257.

Li, S. Y., and C. T. Yue, 2003, Study of pyrolysis kinetics of oil shale: Fuel, v. 82, p. 337-342.

Natural Resources Authority, 2007, Oil Shale – Fact Sheet 2, http://www.nra.gov.jo/index.php. Accessed May 20, 2007.

Nazzal, J. M., 2002, Influence of heating rate on the pyrolysis of Jordan oil shale: Journal of Analytical and Applied Pyrolysis, v. 62, p. 225-238.

Ots, A., 2004, Oil Shale Fuel Combustion, Trukitud Tallinna Raanatutrukikojas, Estonia.

Qing, W., S. Baizhong, H. Aijuan, B. Jingru, and L. Shaohua, 2007, Pyrolysis characteristics of Huadian oil shales: Oil Shale, v. 24, p. 147-157.

Skala, D., H. Kopsch, M. Sokic, H. J. Neumann, and J. Jovanovic, 1987, Thermogravimetrically and differential scanning calorimetrically derived kinetics of oil-shale pyrolysis: Fuel, v. 66, p. 1185-1191.

Skala, D., H. Kopsch, M. Sokic, H. J. Neumann, and J. A. Jovanovic, 1990, Kinetics and modeling of oil-shale pyrolysis: Fuel, v. 69, p. 490-496.

Torrente, M. C., and M. A. Galan, 2001, Kinetics of the thermal decomposition of oil shale from Puertollano (Spain): Fuel, v. 80, p. 327-334.

Wall, L. A., J. H. Flynn, and S. Straus, 1970, Rates of Molecular Vaporization of Linear Alkanes: Journal of Physical Chemistry, v. 74.

Young, D. K., and T. F. Yen, 1977, The nature of straight-chain aliphatic structures in Green River kerogen: Geochimica et Cosmochimica Acta, v. 41, p. 1411-1417.